Metastable and unstable structures in microphase separated diblock copolymers

2005 J. Phys.: Condens. Matter 17 4877

(http://iopscience.iop.org/0953-8984/17/32/002)

INSTITUTE OF PHYSICS PUBLISHING JOURNAL OF PHYSICS: CONDENSED MATTER

J. Phys.: Condens. Matter **17** (2005) 4877–4887 doi:10.1088/0953-8984/17/32/002

Metastable and unstable structures in microphase separated diblock copolymers

Kohtaro Yamada[1,2], **Makiko Nonomura**[1], **Akira Saeki**[3] **and Takao Ohta**[2,4]

[1] Department of Mathematical and Life Sciences, Graduate School of Science, Hiroshima University, Higashi-Hiroshima, 739-8526, Japan
[2] Yukawa Institute for Theoretical Physics, Kyoto University, Kyoto 606-8502, Japan
[3] Department of Physics, Keio University, Yokohama 223-8522, Japan

E-mail: takao@yukawa.kyoto-u.ac.jp

Received 12 May 2005, in final form 19 July 2005
Published 29 July 2005
Online at stacks.iop.org/JPhysCM/17/4877

Abstract

We investigate possible intermediate structures in the process of microphase separation in diblock copolymers. By employing the two-mode expansion valid in the weak-segregation regime, we have found that the $Fddd$ structure and diamond structure of interconnected domains can be metastable whereas the hexagonally perforated lamellar structure and FCC structure exist as a saddle point of the free energy landscape and hence these are unstable.

(Some figures in this article are in colour only in the electronic version)

1. Introduction

Block copolymers self-assemble into a variety of fascinating mesoscopic morphologies. The most typical block copolymers are linear AB-type diblock copolymers. Four equilibrium structures, body-centred-cubic (BCC) spheres, hexagonally packed cylinders, gyroid, and lamellar structures, have been reported both theoretically [1, 2] and experimentally [3].

Apart from these thermal equilibrium structures, it is possible to observe some metastable morphologies. For example, external shear can induce hexagonally perforated layers phase as a metastable structure in a diblock copolymer system [4]. A similar structure has been observed in a water–surfactant mixture in the process of the transition between gyroid and lamellar structures [5].

In our previous paper [6], we studied the kinetics of morphological transitions by using a two-mode expansion with the gyroid symmetry for the local concentration field. The time-evolution of domain structures was analysed in the process of the structural transition between

[4] Author to whom any correspondence should be addressed.

microphase separated phases in the weak-segregation regime. It was also confirmed that several intermediate structures appear during the transitions.

The two-mode expansion is sufficient to express the four equilibrium structures observed in the weak-segregation regime. However, one cannot exclude the possibility that structures with other symmetries appear during the morphological transitions. The most conceivable symmetry is the face centred-cubic (FCC) symmetry since Matsen and Bates have reported that there is a narrow region in the phase diagram where the structure of close-packed spheres is stable [1], even though there have been no experiments, to our knowledge, that have shown that the FCC structure is stable in diblock copolymer melts.

The purpose of the present paper is to explore the possible intermediate structures and their stability within the two-mode expansion method, extending it to cover FCC symmetry. This kind of study (although limited to the weak-segregation regime) has not been available so far, and would be of great importance in understanding the fundamental properties of morphological transitions, such as the transition path of the interconnected mesoscopic structures which are not seen in ordinary structural transitions in solids.

In the next section, we start with the kinetic equation and briefly describe the method of the two-mode expansion. In section 3, we summarize the structures and stability having BCC symmetry, whereas the morphologies with FCC symmetry are described in section 4. The discussion is given in section 5.

2. Kinetic equation and mode expansion

In an AB-type diblock copolymer system, it is well known that the free energy function is given by [7, 8]

$$F\{\phi\} = \int \mathrm{d}\vec{r}\left[\frac{1}{2}(\nabla\phi)^2 - \frac{\tau}{2}\phi^2 + \frac{g}{4}\phi^4\right] + \frac{\alpha}{2}\int \mathrm{d}\vec{r}\int \mathrm{d}\vec{r}'\, G(\vec{r},\vec{r}')\left(\phi(\vec{r}) - \bar{\phi}\right)\left(\phi(\vec{r}') - \bar{\phi}\right), \tag{1}$$

where the order parameter ϕ denotes the difference of the local volume fraction between A monomers and B monomers, i.e. $\phi = \phi_{\mathrm{A}} - \phi_{\mathrm{B}}$, where ϕ_{A} (ϕ_{B}) is the local volume fraction of the A (B) monomers. The incompressibility condition $\phi_{\mathrm{A}} + \phi_{\mathrm{B}} = 1$ has been imposed. The parameters g and α are positive constants. The coefficient τ is inversely proportional to the temperature through the Flory–Huggins parameter χ as $\tau \propto \chi N$, where N is the degree of polymerization. The spatial average of ϕ is denoted by $\bar{\phi}$ and $G(\vec{r},\vec{r}')$ is defined through the relation

$$-\nabla^2 G(\vec{r},\vec{r}') = \delta(\vec{r} - \vec{r}'). \tag{2}$$

Since ϕ is a conserved quantity, its time evolution is given by

$$\frac{\partial\phi}{\partial t} = \nabla^2\frac{\delta F}{\delta\phi}. \tag{3}$$

Substituting (1) into (3), we obtain the kinetics equation [9]

$$\frac{\partial\phi}{\partial t} = \nabla^2\left[-\nabla^2\phi - \tau\phi + g\phi^3\right] - \alpha\left(\phi - \bar{\phi}\right). \tag{4}$$

In our previous paper [6], we employed a mode-expansion method to investigate kinetics of morphological transitions in three dimensions. To make the present paper self-contained, we shall describe the method briefly.

We consider the weak-segregation limit and expand ϕ as follows:

$$\phi(\vec{r},t) = \bar{\phi} + \left[\sum_{l=1}^{12} a_l(t)\mathrm{e}^{\mathrm{i}\vec{q}_l\cdot\vec{r}} + \sum_{m=1}^{6} b_m(t)\mathrm{e}^{\mathrm{i}\vec{p}_m\cdot\vec{r}} + \sum_{n=1}^{12} c_n(t)\mathrm{e}^{\mathrm{i}\vec{k}_n\cdot\vec{r}} + \mathrm{c.c.}\right], \tag{5}$$

where $a_l(t)$, $b_m(t)$ and $c_n(t)$ are real amplitudes and c.c. means complex conjugate. The 30 reciprocal lattice vectors, $\vec{q}_l$, $\vec{p}_m$ and $\vec{k}_n$, are given by

$$\begin{aligned}
&\vec{q}_1 = C_Q(2,-1,1) && \vec{q}_2 = C_Q(-2,1,1)\\
&\vec{q}_3 = C_Q(-2,-1,1) && \vec{q}_4 = C_Q(2,1,1)\\
&\vec{q}_5 = C_Q(-1,-2,1) && \vec{q}_6 = C_Q(1,-2,1)\\
&\vec{q}_7 = C_Q(-1,2,1) && \vec{q}_8 = C_Q(1,2,1)\\
&\vec{q}_9 = C_Q(1,-1,-2) && \vec{q}_{10} = C_Q(1,1,-2)\\
&\vec{q}_{11} = C_Q(-1,1,-2) && \vec{q}_{12} = C_Q(-1,-1,-2)\\
&\vec{p}_1 = C_P(2,2,0) && \vec{p}_2 = C_P(2,-2,0)\\
&\vec{p}_3 = C_P(0,2,2) && \vec{p}_4 = C_P(0,-2,2)\\
&\vec{p}_5 = C_P(2,0,2) && \vec{p}_6 = C_P(-2,0,2)\\
&\vec{k}_1 = C_Q(-w,-w+1,w+1) && \vec{k}_2 = C_Q(w-1,w+1,w)\\
&\vec{k}_3 = C_Q(w,-w-1,w-1) && \vec{k}_4 = C_Q(-w+1,w,w+1)\\
&\vec{k}_5 = C_Q(-w,w+1,w-1) && \vec{k}_6 = C_Q(w,w-1,w+1)\\
&\vec{k}_7 = C_Q(-w-1,-w,w-1) && \vec{k}_8 = C_Q(w-1,-w,w+1)\\
&\vec{k}_9 = C_Q(w+1,-w+1,w) && \vec{k}_{10} = C_Q(w+1,w,w-1)\\
&\vec{k}_{11} = C_Q(-w-1,w-1,w) && \vec{k}_{12} = C_Q(-w+1,-w-1,w),
\end{aligned} \tag{6}$$

where $w = 2\sqrt{3}/3$, $C_Q = Q/\sqrt{6}$ and $C_P = P/(2\sqrt{2})$. The magnitudes P and Q satisfy the following relation:

$$Q^2 = \tfrac{3}{4}P^2. \tag{7}$$

The expression (5) with the vectors given by (6) can describe all the equilibrium structures observed in the weak-segregation regime (i.e. lamellar, hexagonal, BCC and gyroid structures).

Substituting (5) into (4) and ignoring the higher harmonics, we obtain a coupled set of equations for the amplitudes. This method is justified in the weak-segregation limit. Because the amplitude equations are lengthy, we write down only the equation for a_1.

$$\begin{aligned}
\frac{\mathrm{d}a_1}{\mathrm{d}t} = {} & \left(-Q^4 + \tau Q^2 - \alpha\right) a_1 - g Q^2 \Bigg[3\left(\bar{\phi}^2 - {a_1}^2\right) a_1 + 6\Bigg(\sum_{l=1}^{12} {a_l}^2 + \sum_{m=1}^{6} {b_m}^2 + \sum_{n=1}^{12} {c_n}^2\Bigg) a_1 \\
& + 6\big(\bar{\phi} a_3 b_4 + \bar{\phi} a_7 a_{12} + \bar{\phi} c_7 c_{12} + a_1 b_2 b_5 + a_2 a_3 a_4 + a_2 a_5 a_8 + a_2 a_6 a_7 + a_3 b_1 b_2 \\
& + a_3 b_1 b_5 + a_3 b_2 b_6 + a_3 b_5 b_6 + a_4 a_9 a_{10} + a_4 a_{11} a_{12} + a_5 a_{10} b_2 + a_5 a_{10} b_5 \\
& + a_5 a_{12} b_6 + a_6 a_9 b_3 + a_6 a_9 b_6 + a_6 a_{11} b_2 + a_6 a_{11} b_4 + a_6 a_{11} b_5 + a_7 a_{10} b_1 \\
& + a_7 c_1 c_7 + a_8 a_9 b_4 + a_8 a_{11} b_1 + a_8 a_{11} b_3 + a_{12} c_1 c_{12} + b_4 c_8 c_9\big)\Bigg].
\end{aligned} \tag{8}$$

Similarly, substituting (5) into (1), we obtain the free energy function F in the terms of a_l, b_m, c_n, Q and P. All of the amplitude equations and the free energy have been listed in [6].

Since the period of a gyroid structure slightly differs from that of the other equilibrium structures, the wavenumbers, P and Q, should be time-dependent during the morphological transition between a gyroid and other equilibrium structures. However, because we have no systematic way to derive the equation for P (or Q) at present, we employ the relaxation dynamics for the wavenumber:

$$\frac{\mathrm{d}P^2}{\mathrm{d}t} = -h\frac{\partial F}{\partial P^2}, \tag{9}$$

where h is a positive constant.

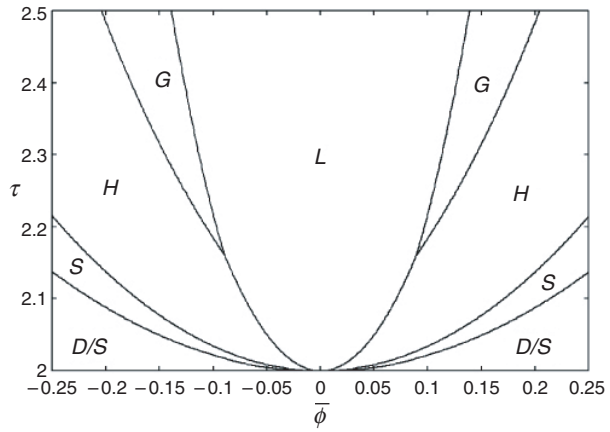

Figure 1. Phase diagram of the τ–$\bar{\phi}$ plane. The regions indicated by L, H, G, and S are the stable phase of lamellae, hexagons, gyroid, and BCC, respectively. DIS means a disorder phase.

From the equilibrium solutions of (8) and (9), we have obtained the phase diagram on the τ–$\bar{\phi}$ plane shown in figure 1 [6]. Other parameters are set to be $\alpha = g = h = 1$. In this case, the order–disorder transition occurs at $\tau = \tau_c = 2$ for $\bar{\phi} = 0$. This critical value should be compared with the mean field critical point $(\chi N)_c = 10.495$ in [2]. We have verified by solving (4) numerically that the concentration variation of monomers is almost sinusoidal, at least up to $\tau/\tau_c = 1.25$, and hence that the mode expansion method is justified. This is the reason why the phase diagram is shown for $2 < \tau < 2.5$, above which the present approximation becomes less accurate.

3. BCC symmetry

In order to investigate the morphological transition, we carried out numerical simulations for the amplitude equations such as (8) and the time-evolution equation for the wavenumber (9), and we found two intermediate structures, the $Fddd$ structure and the perforated lamellar structure [6]. The purpose of this section is to give a full account of these structures which basically belong to BCC symmetry.

In figure 2, the $Fddd$ structure is displayed by the isosurface of ϕ viewed from various directions. This structure appears during the morphological transition from lamellar, hexagonal and BCC structures to a gyroid structure, and from a gyroid structure to a lamellar structure. Furthermore, we have verified that the $Fddd$ structure is one of the equilibrium solutions of the amplitude equations.

The connection of domains and the Bragg points of the $Fddd$ structure are displayed in figures 3(a) and (b), respectively. As seen in figure 3(b), the Bragg points of the $Fddd$ structure form a non-proper hexagon and two rectangles below and above the hexagon. In figure 4, we compare the equilibrium free energy of lamellar, hexagonal, BCC, gyroid and $Fddd$ structures for $\tau = 2.2$. Note that the free energy of the $Fddd$ structure is fairly close to (but larger than) that of a gyroid structure around at $\bar{\phi} \cong 0.1$ where the gyroid structure is most stable. Therefore, the $Fddd$ structure is a metastable structure. It is mentioned that the $Fddd$ structure has been obtained by direct numerical simulations of (4) [10]. Experimentally, the $Fddd$ structure has not been found in AB diblock copolymers but it has been observed in ABC triblock copolymers as an equilibrium phase [11, 12].

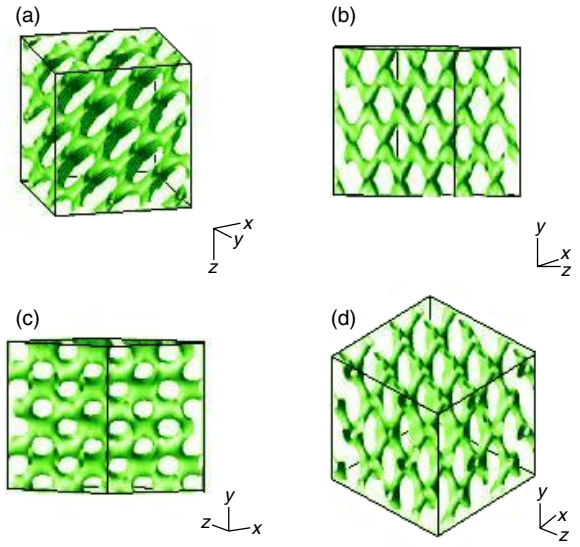

Figure 2. $Fddd$ structure obtained for the parameters $\alpha = g = h = 1$, $\tau = 2.3$ and $\bar{\phi} = -0.05$.

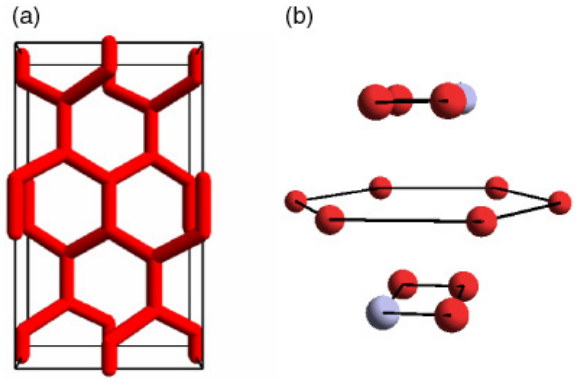

Figure 3. (a) Connection of domains in the $Fddd$ structure. (b) Bragg points of the $Fddd$ structure. The points in the same plane are connected with lines and the white points represent the Bragg points of a lamellar structure.

Next, we discuss the perforated lamellar structure shown in figure 5. This structure appears during the transition from a lamellar structure to a hexagonal structure. This perforated lamellar structure is not a metastable structure, but a transient structure. That is, this structure is not a stable equilibrium solution of the amplitude equations in contrast to the $Fddd$ structure. Qi and Wang have also found this structure by using the single-mode approximation method [13], which is consistent with the present results obtained by the two-mode approximation.

We have examined the position of holes in each layer of the perforated lamellar structure. The figures from left to right in figure 5(b) display the top-view of successive three layers. It is evident from this figure that the holes locate at the same position every two layers. In addition, it is found that the configuration of holes has a rhombic rather than a hexagonal symmetry. Therefore the holes of this perforated lamellar structure are not close-packed. The origin of this might come from the fact that a hexagonally close-packed structure cannot be represented by the mode expansion as long as the number of the modes is finite.

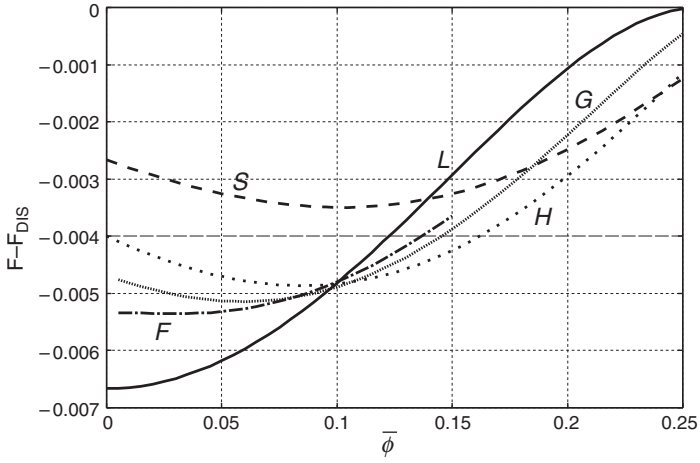

Figure 4. Free energy of lamellar (L), hexagonal (H), BCC (S), gyroid (G) and $Fddd$ (F) structures for $\tau = 2.2$. F_{DIS} is the free energy of a homogeneous state.

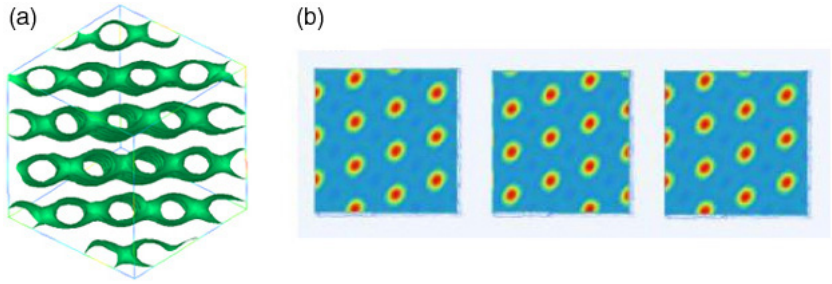

Figure 5. (a) The perforated lamellar structure obtained during the morphological transition from a lamellar structure for $\tau = 2.5$ and $\bar{\phi} = -0.13$ to a hexagonal structure for $\tau = 2.1$ and $\bar{\phi} = -0.13$. (b) The position of holes on each successive layer of the perforated lamellae.

4. FCC symmetry

In the preceding section, we have examined the existence and the stability of the intermediate structures in the morphological transitions based on the expansion (5). However, this mode expansion does not take account of FCC symmetry and its related structures. In this section, in order to investigate the stability of the structures with FCC symmetry, we expand the order parameter ϕ as

$$\phi(\vec{r}, t) = \bar{\phi} + \left[\sum_{m=1}^{4} A_m(t) \mathrm{e}^{\mathrm{i}\vec{s}_m \cdot \vec{r}} + \mathrm{c.c.}\right], \tag{10}$$

where $\vec{s}_m$ are the fundamental reciprocal lattice vectors of the FCC structure and are given by

$$\begin{aligned} \vec{s}_1 &= \frac{S}{\sqrt{3}}(1, 1, 1) \qquad \vec{s}_2 = \frac{S}{\sqrt{3}}(1, -1, 1) \\ \vec{s}_3 &= \frac{S}{\sqrt{3}}(-1, 1, 1) \qquad \vec{s}_4 = \frac{S}{\sqrt{3}}(-1, -1, 1). \end{aligned} \tag{11}$$

The positive constant S is the magnitude of $\vec{s}_m$. Substituting (10) into (4) and ignoring the higher harmonics, we obtain the following set of amplitude equations:

$$\begin{aligned}
\frac{\mathrm{d}A_1}{\mathrm{d}t} &= \left(-S^4+\tau S^2-\alpha\right)A_1 \\
&\quad -3gS^2\left(\bar{\phi}^2A_1+{A_1}^3+2A_1{A_2}^2+2A_1{A_3}^2+2A_1{A_4}^2+2A_2A_3A_4\right) \\
\frac{\mathrm{d}A_2}{\mathrm{d}t} &= \left(-S^4+\tau S^2-\alpha\right)A_2 \\
&\quad -3gS^2\left(\bar{\phi}^2A_2+{A_2}^3+2A_2{A_1}^2+2A_2{A_3}^2+2A_2{A_4}^2+2A_1A_3A_4\right) \\
\frac{\mathrm{d}A_3}{\mathrm{d}t} &= \left(-S^4+\tau S^2-\alpha\right)A_3 \\
&\quad -3gS^2\left(\bar{\phi}^2A_3+{A_3}^3+2A_3{A_1}^2+2A_3{A_2}^2+2A_3{A_4}^2+2A_1A_2A_4\right) \\
\frac{\mathrm{d}A_4}{\mathrm{d}t} &= \left(-S^4+\tau S^2-\alpha\right)A_4 \\
&\quad -3gS^2\left(\bar{\phi}^2A_4+{A_4}^3+2A_4{A_1}^2+2A_4{A_2}^2+2A_4{A_3}^2+2A_1A_2A_3\right).
\end{aligned} \tag{12}$$

The free energy (1) can also be written in terms of the amplitudes as

$$\begin{aligned}
F &= F_{\mathrm{DIS}}+\left(S^2-\tau+\frac{\alpha}{S^2}\right)\sum_{m=1}^{4}{A_m}^2 \\
&\quad +\frac{3g}{2}\left(-\sum_{m=1}^{4}{A_m}^4+2\sum_{m=1}^{4}\sum_{n=1}^{4}{A_m}^2{A_n}^2+8A_1A_2A_3A_4+2\bar{\phi}^2\sum_{m=1}^{4}{A_m}^2\right),
\end{aligned} \tag{13}$$

where F_{DIS} is the free energy of the homogeneous state given by

$$F_{\mathrm{DIS}}=-\frac{\tau}{2}\bar{\phi}^2+\frac{g}{4}\bar{\phi}^4. \tag{14}$$

We have solved (12) numerically and found that there are two types of equilibrium solution. One is given by the set $A_1=A$ and $A_2=A_3=A_4=B$, and the other is given by $A_1=A_2=C$ and $A_3=A_4=D$. We shall examine the stability of each solution below.

First, we consider the case $A_1=A$ and $A_2=A_3=A_4=B$ where (12) can be simplified as

$$\begin{aligned}
\frac{\mathrm{d}A}{\mathrm{d}t} &= \left(-S^4+\tau S^2-\alpha\right)A-3gS^2\left(A^3+6AB^2+2B^3+\bar{\phi}^2A\right) \\
\frac{\mathrm{d}B}{\mathrm{d}t} &= \left(-S^4+\tau S^2-\alpha\right)B-3gS^2\left(5B^3+2AB^2+2A^2B+\bar{\phi}^2B\right).
\end{aligned} \tag{15}$$

The nullclines of (15) for $\alpha=g=1$, $\tau=2.2$ and $\bar{\phi}=0.1$ are shown in figure 6, where an S-shaped curve indicates the line $\mathrm{d}A/\mathrm{d}t=0$ and a slanted ellipse and a horizontal line represent the lines given by $\mathrm{d}B/\mathrm{d}t=0$. Two diagonal lines indicate the lines $A=\pm B$. The circles and squares at the intersection of the curves $\mathrm{d}A/\mathrm{d}t=0$ and $\mathrm{d}B/\mathrm{d}t=0$ indicate the stable and unstable solutions, respectively.

In this case, there are five solutions characterized by l, f, d, p and o as indicated in figure 6. The solutions l given by $A\neq 0$ and $B=0$ and o given by $A=B=0$ indicate a lamellar structure and a disorder state, respectively. The lamellar structure is stable whereas the disorder state is unstable with this parameter set. From the expansion of ϕ (10), one can easily find that the solution f, that is $A=B\neq 0$, is an FCC structure. It is emphasized that this FCC structure is unstable. On the other hand, it has been reported that close-packed spheres (either FCC structure or hexagonally close-packed structure) exist as a stable equilibrium structure above a certain degree of segregation [1]. This discrepancy might be attributed to the condition that our study is restricted to the weak-segregation regime. In fact, as mentioned at the end of

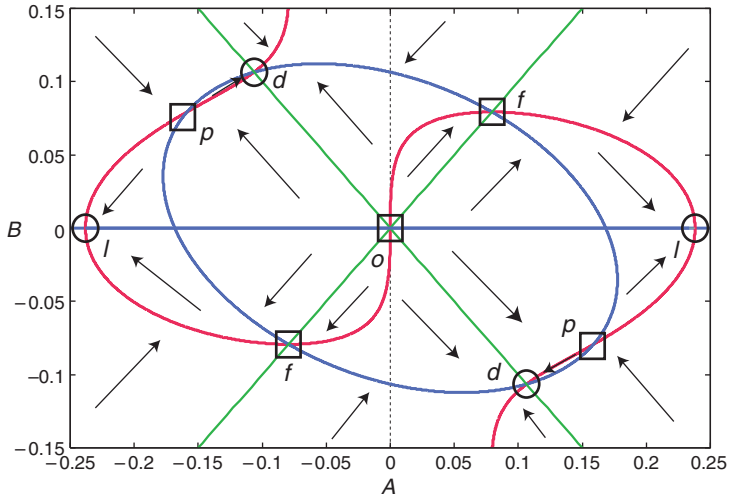

Figure 6. The nullclines of (15) for $\alpha = g = 1$, $\tau = 2.2$ and $\bar{\phi} = 0.1$. An S-shaped curve indicates the line $\mathrm{d}A/\mathrm{d}t = 0$ and a slanted ellipse and a horizontal line represent the lines given by $\mathrm{d}B/\mathrm{d}t = 0$. Two diagonal lines indicate the equality $A = B$ and $-B$. The direction of the arrows indicates the direction of $\mathrm{d}A/\mathrm{d}t$ and $\mathrm{d}B/\mathrm{d}t$. The solutions of lamellar, FCC, diamond, hexagonally perforated lamellar and disorder structures are indicated by l, f, d, p and o, respectively. The solutions shown by the circles are stable, whereas those by the squares are unstable.

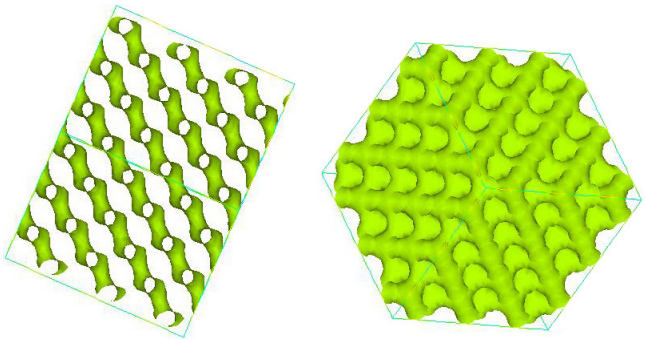

Figure 7. View from the [110] direction (left) and from the [111] direction (right) of hexagonally perforated lamellar structure marked as p in figure 6.

section 2, the present theory is valid for $\tau/\tau_c \leqslant 1.25$, whereas the results in [2] indicate that a close-packed structure appears in the phase diagram for $\chi N/(\chi N)_c \geqslant 1.7$.

The structure of the solution p, i.e. $A \neq 0$, $B \neq 0$ and $A \neq B$, corresponds to a perforated lamellar structure as shown in figure 7. Figure 8 clarifies that these holes are arrayed hexagonally in each layer and located at the same position every three layers. From these facts, one can easily identify it with a hexagonally perforated lamellar structure (ABC type) with a close-packed structure of holes. Note that this perforated lamellar structure is unstable as well as another perforated lamellae (AB-type) discussed in section 3.

We identify the solution d in figure 6 with a diamond structure which is shown in figure 9. It is noted that the diamond structure is stable with respect to deviations of the amplitudes A_i $(i = 1, \ldots, 4)$ around the equilibrium value.

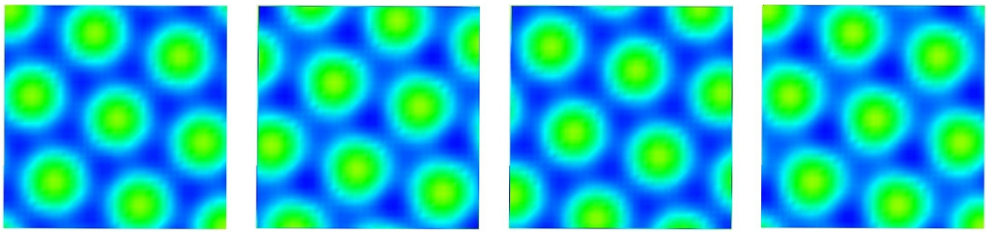

Figure 8. Position of holes on each successive layer of the hexagonally perforated lamellar structure. The majority component exists more than the minority one at the circular regions.

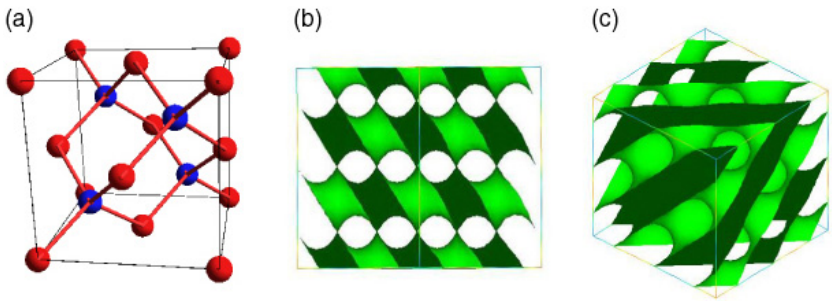

Figure 9. (a) Diamond structure. The four junctions are inside the unit cubic cell whereas the remaining junctions are on the faces of the cell. (b) View from the [110] direction (left) and from the [111] direction (right).

Next, we consider the case of $A_1 = A_2 = C$ and $A_3 = A_4 = D$, where (12) can be rewritten as

$$\begin{aligned} \frac{\mathrm{d}C}{\mathrm{d}t} &= \left(-S^4 + \tau S^2 - \alpha\right) C - 3gS^2 \left(3C^3 + 6CD^2 + \bar{\phi}^2 C\right) \\ \frac{\mathrm{d}D}{\mathrm{d}t} &= \left(-S^4 + \tau S^2 - \alpha\right) D - 3gS^2 \left(3D^3 + 6C^2 D + \bar{\phi}^2 D\right). \end{aligned} \tag{16}$$

The nullclines of (16) for $\alpha = g = 1$, $\tau = 2.2$ and $\bar{\phi} = 0.1$ are shown in figure 10. The solutions f and o represent an unstable FCC structure and an unstable homogeneous state, as in the previous case. The stable solution c is given either by $C \neq 0$ and $D = 0$ or by $C = 0$ and $D \neq 0$. Therefore, this structure is represented only by two reciprocal vectors and is essentially a two-dimensional structure. The concentration variation is displayed in figure 11, which indicates a distorted cylindrical structure.

The free energy of these structures for $\tau = 2.2$ is compared to that of a lamellar structure in figure 12. It is evident that the diamond structure and the distorted cylindrical structure are not the most stable structures.

5. Summary and discussion

We have explored the intermediate structures in the process of the morphological transitions by means of the mode expansion approach. By solving the amplitude equations for BCC and FCC symmetries, we have found several time-independent solutions such as $Fddd$, FCC, hexagonally perforated lamellar, perforated lamellar (AB-type) and diamond structures. Among the equilibrium solutions, the $Fddd$ structure, distorted cylindrical structure and

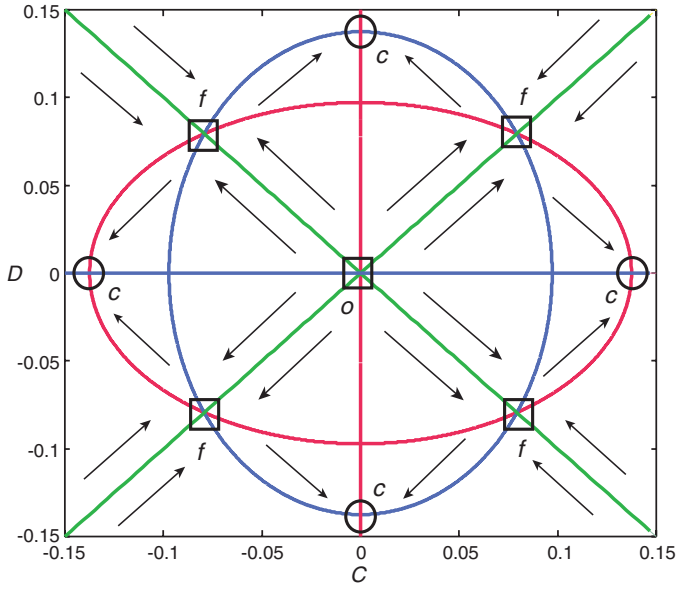

Figure 10. The nullclines of (16) for $\alpha = g = 1$, $\tau = 2.2$ and $\bar{\phi} = 0.1$. An ellipse horizontally (vertically) elongated and a vertical (horizontal) line represent the line $\mathrm{d}C/\mathrm{d}t = 0$ ($\mathrm{d}D/\mathrm{d}t = 0$). Two diagonal lines indicate $C = D$ and $-D$. The equilibrium solutions are c, f and o.

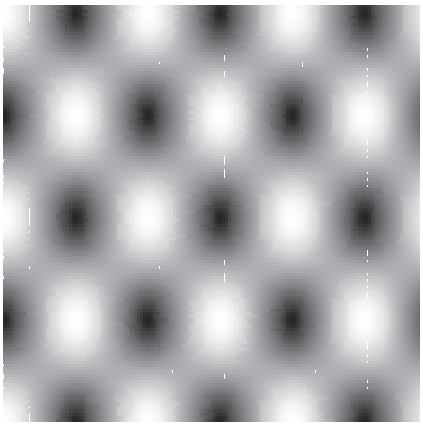

Figure 11. Distorted cylindrical structure marked as c in figure 10.

diamond structure are stable within the two-mode theory. The equilibrium free energies of the distorted cylinders and the diamond structure are higher than that of the lamellar structure, and that of the $Fddd$ structure is higher than those of the hexagonal and lamellar structures. Therefore these are candidates for a metastable structure in the course of morphological transitions. In our previous study [6], the $Fddd$ structure indeed appears as an intermediate structure in the transition.

On the other hand, the FCC structure, hexagonally perforated lamellar structure and AB-type of perforated lamellar structure are unstable solutions of the amplitude equations valid in the weak-segregation regime. Although these are unstable, we do not exclude the possibility

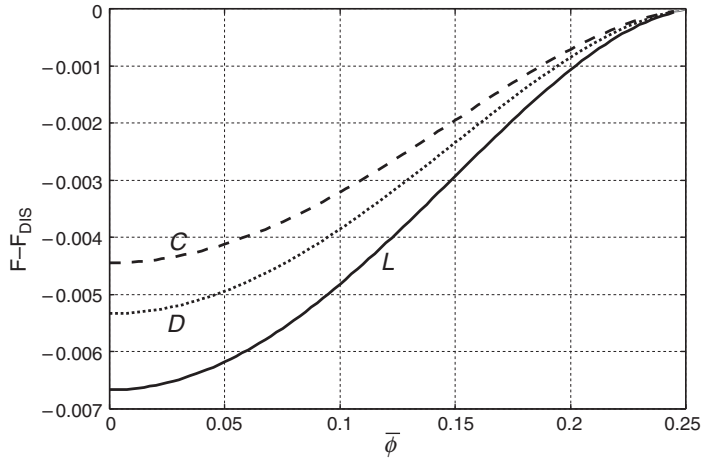

Figure 12. Comparison of the free energy of lamellar (L), cylindrical (C) and diamond (D) structures for $\tau = 2.2$. It should be noted that there is a region for $\bar{\phi} \geqslant 0.1$ where gyroid, hexagonal, and bcc structures are more stable than the lamellar structure, as shown in figure 4.

that the structures are observed in the transition kinetics as a transient morphology, because the solutions are the saddle points of the free energy landscape.

It is an interesting future work to investigate the stability of these structures under external fields, such as shear flow and electric field, where some of the unstable or metastable structures might become more stable. Solvent effects would also alter the stability. These extensions of the present approach will be useful to obtain insight into the domain control of mesoscopic structures.

Acknowledgments

This work was supported by the Grant-in-Aid of the Ministry of Education, Science and Culture of Japan and by a Grant-in-Aid for the 21st Century COE 'Center for Diversity and Universality in Physics'.

References

[1] Matsen M W and Bates F S 1996 *Macromolecules* **29** 7641
[2] Matsen M W and Bates F S 1996 *Macromolecules* **29** 1091
[3] Khandpur A K, Forster S, Bates F S, Hamley I W, Ryan A J, Bras W, Almdal K and Mortensen K 1995 *Macromolecules* **28** 8796
[4] Zhu L, Huang P, Chen W Y, Weng X, Cheng X S Z D, Ge Q, Quirk R P, Senador T, Shaw M T, Thomas E L, Lots B, Hsiao B S, Yeh F and Liu L 2003 *Macromolecules* **36** 3180
[5] Imai M, Saeki A, Teramoto T, Kawaguchi A, Nakaya K, Kato T and Ito K 2001 *J. Chem. Phys.* **115** 10525
[6] Yamada K, Nonomura M and Ohta T 2004 *Macromolecules* **37** 5762
[7] Ohta T and Kawasaki K 1986 *Macromolecules* **19** 2621
[8] Ohta T and Kawasaki K 1990 *Macromolecules* **23** 2413
[9] Bahiana M and Oono Y 1990 *Phys. Rev.* A **41** 6763
[10] Nonomura M and Ohta T 2001 *J. Phys.: Condens. Matter* **13** 9089
[11] Bailey T S, Hardy C M, Epps T H III and Bates F S 2002 *Macromolecules* **35** 7007
[12] Epps T H III, Bailey T S, Waletzko R and Bates F S 2003 *Macromolecules* **36** 2873
[13] Qi S and Wang Z G 1997 *Phys. Rev.* E **55** 1682